MENU 2007
11th International Conference
on Meson-Nucleon Physics and
the Structure of the Nucleon
September10-14, 2007
IKP, Forschungzentrum Jülich, Germany

COULOMB EFFECTS IN FEW-NUCLEON SYSTEMS

A. C. Fonseca
Centro de Física Nuclear da Universidade de Lisboa
Av. Prof. Gama Pinto 2, P-1649-003 Lisboa, Portugal

Abstract

Recent progress on the solution of *ab initio* three- and four-nucleon scattering equations in momentum space that include the correct treatment of the Coulomb interaction is reviewed; results for specific observables in reactions initiated by $p + d$, $p + {}^3\mathrm{He}$ and $n + {}^3\mathrm{He}$ are shown.

1 Introduction

In recent years considerable progress has been achieved in the study of nuclei up to $A \leq 12$ through *ab initio* structure calculations based on the underlying concept that nucleons interact through pairwise forces fitted to nucleon-nucleon (NN) scattering up to the pion production threshold plus a three-nucleon force [1, 2] when necessary. The same concept applies to *ab initio* scattering calculations but here restricted to three- [3, 4] or four-nucleon [5–7] reactions given the greater difficulty involved in the solution of many-body scattering equations, particularly in the presence of the repulsive Coulomb force between charged protons.

In the present review we account for the changes that have taken place since 2005, leading to fully converged *ab initio* calculations of $p + d$ elastic scattering and breakup at energies up to the pion production threshold and all possible four-nucleon reactions initiated by $n + {}^3\mathrm{He}$, $p + {}^3\mathrm{H}$, $d + d$, $n + {}^3\mathrm{H}$ and $p + {}^3\mathrm{He}$ below three-body breakup threshold.

2 Three-Nucleon Scattering with Two Protons

The treatment of the Coulomb interaction is based on the ideas proposed in Ref. [8] for the scattering of two charged particles and extended in Ref. [9]

for three-particle scattering. The Coulomb potential is screened, standard scattering theory for short-range potentials is used and the obtained results are corrected for the unscreened limit through the renormalization method proposed in Refs. [8,9]. Although the theory was well established, no reliable calculations existed due to the shortcomings of the practical implementation. In Refs. [10,11] we have demonstrated how one obtains fully converged calculations for p+d elastic scattering and breakup, p+d capture into ^{3}He+γ, and two- and three-body photo and electro disintegration using realistic nucleon-nucleon interactions plus the Coulomb potential between protons.

One major difference relative to previous work is that we use a Coulomb potential w_R, screened around the separation $r = R$ between two charged baryons which, in configuration space, reads

$$w_R(r) = w(r)\; e^{-(r/R)^n}, \tag{1}$$

with the true Coulomb potential $w(r) = \alpha_e/r$, where $\alpha_e \approx 1/137$ is the fine structure constant and n controls the smoothness of the screening. We prefer to work with a sharper screening than the Yukawa screening ($n = 1$) of Ref. [9]. We want to ensure that the screened Coulomb potential w_R approximates well the true Coulomb one w for distances $r < R$ and simultaneously vanishes rapidly for $r > R$, providing a comparatively fast convergence of the partial-wave expansion. In contrast, the sharp cutoff ($n \to \infty$) yields an unpleasant oscillatory behavior in the momentum-space representation, leading to convergence problems. We find that values $3 \leq n \leq 6$ provide a sufficiently smooth, but at the same time a sufficiently rapid screening around $r = R$.

In addition to a different choice of screening function, our calculations are based on the definition of a "two-potential formula" where one separates the long range Coulomb amplitude between the proton and the center of mass (c.m.) of the deuteron from the remainder that constitutes the Coulomb modified short range contribution to the full scattering amplitude.

The starting point in our approach is the full three-body Alt, Grassberger and Sandhas (AGS) equation [12] for the transition operator $U^{(R)}_{\beta\alpha}(Z)$ that depends parametrically on the screening radius R

$$U^{(R)}_{\beta\alpha}(Z) = \overline{\delta}_{\beta\alpha} G_0^{-1}(Z) + \sum_\sigma \overline{\delta}_{\beta\sigma} T^{(R)}_\sigma(Z) G_0(Z) U^{(R)}_{\sigma\alpha}(Z), \tag{2a}$$

where the two-particle transition matrix $T^{(R)}_\sigma$ is derived from the full channel interaction $v_\alpha + w_{\alpha R}$

$$T^{(R)}_\alpha(Z) = (v_\alpha + w_{\alpha R}) + (v_\alpha + w_{\alpha R}) G_0(Z) T^{(R)}_\alpha(Z), \tag{2b}$$

$G_0(Z) = (Z - H_0)^{-1}$ is the free resolvent and $\overline{\delta}_{\beta\alpha} = 1 - \delta_{\beta\alpha}$. Of course, the full multichannel transition matrix $U^{(R)}_{\beta\alpha}(Z)$ must contain the pure Coulomb transition matrix $T^{\rm c.m.}_{\alpha R}(Z)$ derived from the screened Coulomb potential $W^{\rm c.m.}_{\alpha R}$ between the spectator proton and the center of mass (c.m.) of the remaining neutron-proton pair in channel α, that is,

$$T^{\rm c.m.}_{\alpha R}(Z) = W^{\rm c.m.}_{\alpha R} + W^{\rm c.m.}_{\alpha R} G^{(R)}_{\alpha}(Z) T^{\rm c.m.}_{\alpha R}(Z), \tag{3a}$$

$$G^{(R)}_{\alpha}(Z) = (Z - H_0 - v_\alpha - w_{\alpha R})^{-1}, \tag{3b}$$

with the *pd* channel being one of those channels α. The same screening function is used for both Coulomb potentials $w_{\alpha R}$ and $W^{\rm c.m.}_{\alpha R}$. As shown in [10] $[U^{(R)}_{\beta\alpha}(Z) - \delta_{\beta\alpha} T^{\rm c.m.}_{\alpha R}(Z)]$ is a short range operator which after renormalization [9] has a well defined $R \to \infty$ limit. Therefore, in the $R \to \infty$ limit

$$\begin{aligned} \langle \mathbf{q}_\beta | U_{\beta\alpha} | \mathbf{q}_\alpha \rangle &= \delta_{\beta\alpha} \langle \mathbf{q}_\beta | T^{\rm c.m.}_{\alpha C} | \mathbf{q}_\alpha \rangle \\ &+ \lim_{R\to\infty} (\mathcal{Z}^{-\frac{1}{2}}_{\beta R}(q_\beta) \langle \mathbf{q}_\beta | [U^{(R)}_{\beta\alpha}(Z) - \delta_{\beta\alpha}\, T^{\rm c.m.}_{\alpha R}(Z)] | \mathbf{q}_\alpha \rangle \mathcal{Z}^{-\frac{1}{2}}_{\alpha R}(q_\alpha)), \end{aligned} \tag{4}$$

where

$$\mathcal{Z}_{\alpha R}(q) = e^{-2i(\sigma^\alpha_l(q) - \eta^\alpha_{lR}(q))}, \tag{5}$$

with the diverging screened Coulomb *pd* phase shift $\eta^\alpha_{lR}(q)$ corresponding to standard boundary conditions and the proper Coulomb one $\sigma^\alpha_l(q)$ referring to the logarithmically distorted proper Coulomb boundary conditions; l is the *pd* relative orbital angular momentum. Likewise for breakup we show [10] that

$$\langle \mathbf{p}_f \mathbf{q}_f | U_{0\alpha} | \mathbf{q}_\alpha \rangle = \lim_{R\to\infty} \{ z^{-\frac{1}{2}}_R(p_f) \langle \mathbf{p}_f \mathbf{q}_f | U^{(R)}_{0\alpha}(Z) | \mathbf{q}_\alpha \rangle \mathcal{Z}^{-\frac{1}{2}}_{\alpha R}(q_\alpha) \}, \tag{6}$$

$$U^{(R)}_{0\alpha}(Z) = G^{-1}_0(Z) + \sum_\sigma T^{(R)}_\sigma(Z) G_0(Z) U^{(R)}_{\sigma\alpha}(Z), \tag{7}$$

where $\mathcal{Z}_{\alpha R}(q_\alpha)$ and $z_R(p_f)$ are the corresponding *pd* and *pp* renormalizations factors. Equations (2a), (3a) and (7) are solved independently for each R and the corresponding on-shell amplitudes for nuclear plus Coulomb calculated in the $R \to \infty$ limit through (4) and (6). In effect the convergence with R is obtained at small finite R as demonstrated in Ref. [10, 11] for elastic scattering and breakup. All configurations converge at $R = 20$ fm except the *pp*-FSI configuration where a *pp*-FSI peak in the absence of Coulomb, becomes a *pp*-FSI depression with zero cross section at $E_{pp} = 0$ MeV when Coulomb is added. Although further details may be found in Refs. [10,11] we show in Figs. 1-3 three examples on how Coulomb effects in *pd* breakup and

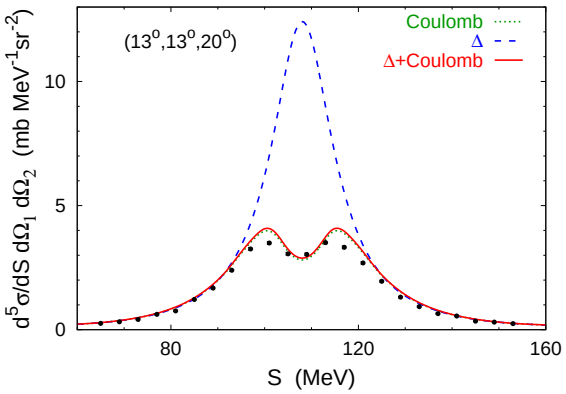

Figure 1: Fivefold differential cross section for dp breakup at $E_d = 130$ MeV close to $pp-$FSI. The solid line corresponds to calculations with CD Bonn + Δ + Coulomb, the dotted line to CD Bonn + Coulomb and the dashed line to CD Bonn + Δ. The dots are data from Ref. [15].

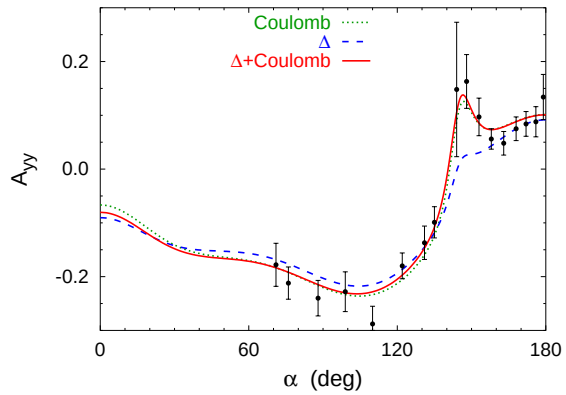

Figure 2: Same as in Fig. 1 for deuteron analyzing power A_{yy} resulting from dp breakup at $E_d = 94.5$ MeV in SCRE geometry. The dots are data from Ref. [16].

three-body photo disintegration of ^{3}He are paramount to describe the data. The calculations are based on the purely nucleonic charge-dependent CD-Bonn potential [13] and its coupled-channel extension, CD-Bonn + Δ [14], allowing for a single virtual Δ - isobar excitation and fitted to the experimental data with the same degree of accuracy as the CD-Bonn itself. In the three-nucleon system the Δ isobar mediates an effective three-nucleon force and effective two- and three-nucleon currents, both consistent with the

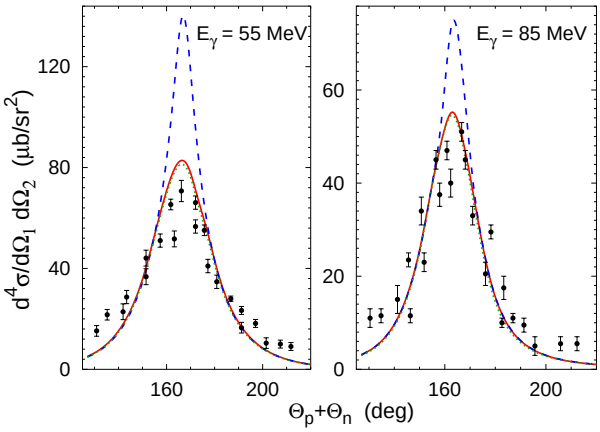

Figure 3: The semi-inclusive fourfold differential cross section for ^{3}He$(\gamma, pn)p$ reaction at 55- and 85-MeV photon lab energy as a function of the np opening angle $\theta_p + \theta_n$ with $\theta_p = 81°$. Curves as in Fig. 1. The experimental data are from Ref. [17].

underlying two-nucleon force.

3 Four-Nucleon Scattering

The four-nucleon ($4N$) scattering problem gives rise to the simplest set of nuclear reactions that shows the complexity of heavier systems. The neutron-^{3}H (n-^{3}H) and proton-^{3}He (p-^{3}He) scattering is dominated by the total isospin $\mathcal{T} = 1$ states while elastic deuteron-deuteron (d-d) scattering by the $\mathcal{T} = 0$ states; the reactions n-^{3}He and p-^{3}H involve both $\mathcal{T} = 0$ and $\mathcal{T} = 1$ and are coupled to d-d in $\mathcal{T} = 0$. Due to the charge dependence of the hadronic and electromagnetic interaction a small admixture of $\mathcal{T} = 2$ states is also present. In $4N$ scattering the Coulomb interaction is paramount not only to treat p-^{3}He but also to separate the n-^{3}He threshold from p-^{3}H and at the same time avoid a second excited state of the α particle a few keV bellow the lowest scattering threshold. All these complex features make the $4N$ scattering problem a natural theoretical laboratory to test different force models of the nuclear interaction, after the $3N$ system [3, 10].

The equations we solve are the four-body AGS equations of Ref. [18] which were used in Ref. [19] to study n-^{3}H elastic scattering and in Ref. [20] to calculate p-^{3}He with the Coulomb force included between all three-protons. As in (2a) the four-body AGS transition operators in the presence of screened Coulomb become R dependent. The transition operators $\mathcal{U}^{\alpha\beta}_{(R)}$ where $\alpha(\beta) = 1$

and 2 corresponds to initial/final $1+3$ and $2+2$ two-cluster states, respectively, satisfy the symmetrized AGS equations

$$\mathcal{U}^{11}_{(R)} = -(G_0\,T^{(R)}G_0)^{-1}P_{34} - P_{34}\,U^1_{(R)}\,G_0\,T^{(R)}G_0\,\mathcal{U}^{11}_{(R)} + U^2_{(R)}G_0\,T^{(R)}G_0\,\mathcal{U}^{21}_{(R)}, \tag{8a}$$

$$\mathcal{U}^{21}_{(R)} = (G_0\,T^{(R)}G_0)^{-1}\,(1-P_{34}) + (1-P_{34})U^1_{(R)}\,G_0\,T^{(R)}G_0\,\mathcal{U}^{11}_{(R)}. \tag{8b}$$

Here G_0 is the four free particle Green's function and $T^{(R)}$ the two-nucleon t-matrix derived from nuclear potential plus screened Coulomb between pp pairs. The operators $U^\alpha_{(R)}$ obtained from

$$U^\alpha_{(R)} = P_\alpha G_0^{-1} + P_\alpha\,T^{(R)}\,G_0\,U^\alpha_{(R)}, \tag{9a}$$

$$P_1 = P_{12}\,P_{23} + P_{13}\,P_{23}, \tag{9b}$$

$$P_2 = P_{13}\,P_{24}, \tag{9c}$$

are the symmetrized AGS operators for the $1+(3)$ and $(2)+(2)$ subsystems and P_{ij} is the permutation operator of particles i and j. Defining the initial/final $1+(3)$ and $(2)+(2)$ states with relative two-body momentum $\mathbf{p}$

$$|\phi^{(R)}_\alpha(\mathbf{p})\rangle = G_0\,T^{(R)}P_\alpha|\phi^{(R)}_\alpha(\mathbf{p})\rangle, \tag{10}$$

the amplitudes for $1+3 \to 1+3$ and $1+3 \to 2+2$ are obtained as $\langle \mathbf{p}_f|T^{\alpha\beta}_{(R)}|\mathbf{p}_i\rangle = S_{\alpha\beta}\langle\phi^{(R)}_\alpha(\mathbf{p}_f)|\mathcal{U}^{\alpha\beta}_{(R)}|\phi^{(R)}_\beta(\mathbf{p}_i)\rangle$ with $S_{11}=3$ and $S_{21}=\sqrt{3}$.

In close analogy with pd elastic scattering, the full scattering amplitude, when calculated between initial and final p-^{3}He states, may be decomposed as follows

$$T^{11}_{(R)} = T^{\rm c.m.}_R + [T^{11}_{(R)} - T^{\rm c.m.}_R], \tag{11}$$

with the long-range part $T^{\rm c.m.}_R$ being the two-body t-matrix derived from the screened Coulomb potential of the form (1) between the proton and the c.m. of ^{3}He, and the remaining Coulomb distorted short-range part $[T^{11}_{(R)} - T^{\rm c.m.}_R]$ as demonstrated before for pd. Applying the renormalization procedure, i.e., multiplying both sides of Eq. (11) by the renormalization factor Z_R^{-1}, in the $R\to\infty$ limit, yields the full $1+3 \to 1+3$ transition amplitude in the presence of Coulomb

$$\langle \mathbf{p}_f|T^{11}|\mathbf{p}_i\rangle = \langle \mathbf{p}_f|T^{\rm c.m.}_C|\mathbf{p}_i\rangle + \lim_{R\to\infty}\left\{\langle \mathbf{p}_f|[T^{11}_{(R)} - T^{\rm c.m.}_R]|\mathbf{p}_i\rangle Z_R^{-1}\right\}. \tag{12}$$

Although the limit in the second term of Eq. (12) is carried out numerically, it is reached for finite R as shown in Fig. 4, where one sees that Coulomb effects are large.

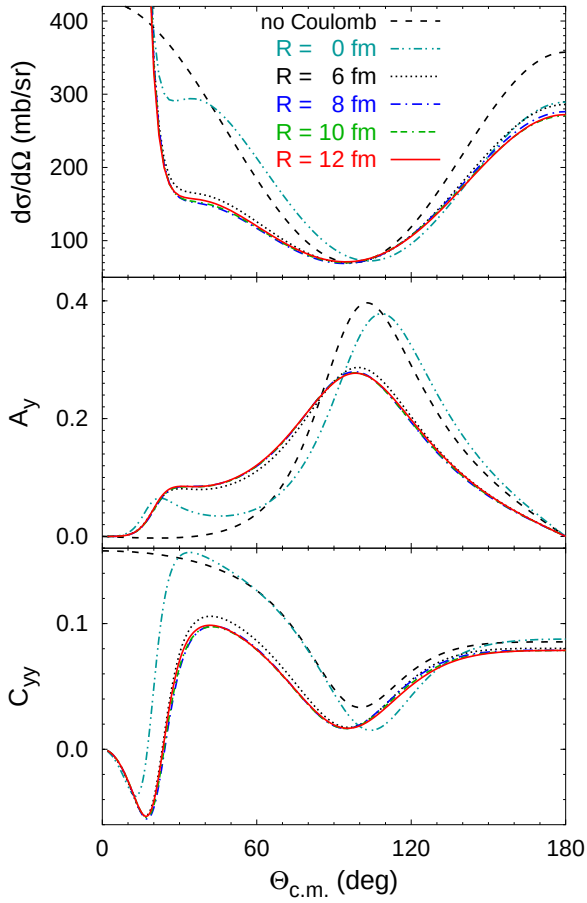

Figure 4: (Color online) Convergence of the p-^{3}He scattering observables with screening radius R. Results for the differential cross section, proton analyzing power A_y, and p-^{3}He spin correlation coefficient C_{yy} at 4 MeV proton lab energy obtained with screening radius $R = 0$ fm (dashed-double-dotted curves), 6 fm (dotted curves), 8 fm (dashed-dotted curves), 10 fm (double-dashed-dotted curves), and 12 fm (solid curves) are compared. Results without Coulomb (dashed curves) are given as reference for the size of the Coulomb effect.

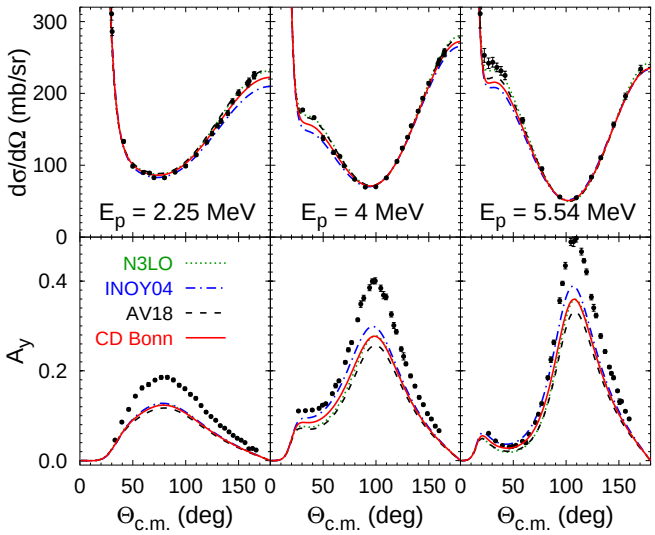

Figure 5: The differential cross section and proton analyzing power A_y of elastic p-^{3}He scattering at 2.25, 4.0, and 5.54 MeV proton lab energy. Results including the Coulomb interaction obtained with potentials CD Bonn (solid curves), AV18 (dashed curves), INOY04 (dashed-dotted curves), and N3LO (dotted curves) are compared. The data are from Refs. [25–27].

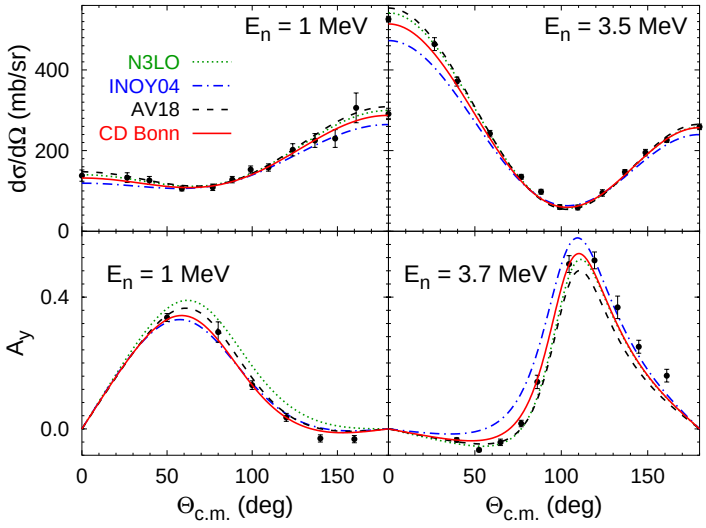

Figure 6: Differential cross section and neutron analyzing power of elastic n-^{3}He scattering at 1, 3.5, and 3.7 MeV neutron lab energy. The curves as in Fig. 5. The cross section data are from Ref. [28], A_y data are from Ref. [29] at 1 MeV and from Ref. [30] at 3.7 MeV.

In Fig. 5-6 we show results for p-^{3}He and n-^{3}He elastic scattering respectively using AV18 [21], CD-Bonn [13], N3LO [22] and INOY04 [23] potentials between NN pairs plus Coulomb. No $3N$ force is included at this time. Results indicate that in p-^{3}He there is a stronger A_y deficiency than in n-^{3}He. This finding may reveal the need for stronger isospin dependent forces but further studies are needed such as including a $3N$ force. Other considerations and examples may be found in Refs. [20] and [24].

4 Conclusions

We have reviewed the most recent work on *ab initio* scattering calculations for three- and four-nucleon reactions using realistic pairwise interactions and the Coulomb force between protons. The calculations with the inclusion of the Coulomb potential are now as accurate as those without, and provide an opportunity for a comprehensive test of hadronic interactions by comparing theory with experimental results obtained with charge particle reactions where data is abundant and error bars smaller.

References

[1] S.C. Pieper, V.R. Pandharipande, R.B. Wiringa and J. Carlson, *Phys. Rev.* **C64**, 014001 (2001).

[2] K. Varga, S.C. Pieper, Y. Suzuki and R.B. Wiringa, *Phys. Rev.* **C66**, 044310 (2002).

[3] W. Glöckle *et al.*, *Phys. Rep.* **274**, 107 (1996).

[4] A. Kievsky, M. Viviani and S. Rosati, *Phys. Rev.* **C64**, 024002 (2001); M. Viviani *et al.*, *Phys. Rev.* **C61**, 064001 (2000).

[5] R. Lazauskas and J. Carbonell, *Phys. Rev.* **C70**, 044002 (2004).

[6] R. Lazauskas *et al.*, *Phys. Rev.* **C71**, 034004 (2005).

[7] M.Viviani *et al.*, *Phys. Rev. Lett.* **86**, 3739 (2001).

[8] J.R. Taylor, *Nuovo Cimento* **B23**, 313 (1974); M.D. Semon and J.R. Taylor, *ibid.* **A26**, 48 (1975).

[9] E.O. Alt, W. Sandhas and H. Ziegelmann, *Phys. Rev.* **C17**, 1981 (1978).

[10] A. Deltuva, A.C. Fonseca and P. U. Sauer, *Phys. Rev.* **C71**, 054005 (2005); **C72**, 054004 (2005); **C73**, 057001 (2006).

[11] A. Deltuva, A.C. Fonseca and P.U. Sauer, *Phys. Rev. Lett.* **95**, 092301 (2005).

[12] E.O. Alt, P. Grassberger and W. Sandhas, *Nucl. Phys.* **B2**, 167 (1967).

[13] R. Machleidt, *Phys. Rev.* **C63**, 024001 (2001).

[14] A. Deltuva, R. Machleidt and P.U. Sauer, *Phys. Rev.* **C68**, 024005 (2003).

[15] St. Kistryn *et al.*, *Phys. Lett.* **B641**, 23 (2006).

[16] D.A. Low *et al.*, *Phys. Rev.* **C44**, 2276 (1991).

[17] N. R. Kolb, P. N. Dezendorf, M. K. Brussel, B. B. Ritchie, and J. H. Smith, *Phys. Rev.* **C44**, 37 (1991).

[18] P. Grassberger and W. Sandhas, *Nucl. Phys.* **B2**, 181 (1967); E. O. Alt, P. Grassberger, and W. Sandhas, JINR report No. E4-6688 (1972).

[19] A. Deltuva and A.C. Fonseca, *Phys. Rev.* **C75**, 014005 (2007).

[20] A. Deltuva and A.C. Fonseca, *Phys. Rev. Lett.* **98**, 162502 (2007).

[21] R. B. Wiringa *et al.*, *Phys. Rev.* **C51**, 38 (1995).

[22] D. R. Entem and R. Machleidt, *Phys. Rev.* **C68**, 041001 (2003).

[23] P. Doleschall, *Phys. Rev.* **C69**, 054001 (2004).

[24] A. Deltuva and A.C. Fonseca, *Phys. Rev.* **C76**, 021001(R) (2007).

[25] B. M. Fisher *et al.*, *Phys. Rev.* **C74**, 034001 (2006).

[26] D. G. McDonald, W. Haeberli, and L. W. Morrow, *Phys. Rev.* **133**, B1178 (1964).

[27] M. T. Alley and L. D. Knutson, *Phys. Rev.* **C48**, 1890 (1993).

[28] J. D. Seagrave, L. Cranberg, and J. E. Simmons, *Phys. Rev.* **119**, 1981 (1960).

[29] P. Jany *et al.*, *Nucl. Phys.* **A483**, 269 (1988).

[30] H. O. Klages *et al.*, *Nucl. Phys.* **A443**, 237 (1985).